# Origin of hydrogen passivation in 4*H*-SiC

Xuefen Cai,[1] Yang Yang,[1] Hui-Xiong Deng,[2,*] and Su-Huai Wei[1,†]
[1]*Beijing Computational Science Research Center, Beijing 100094, China*
[2]*State Key Laboratory of Superlattices and Microstructures, Institute of Semiconductors, Chinese Academy of Sciences, Beijing 100083, China*

(Received 1 March 2021; accepted 9 June 2021; published 22 June 2021)

Carbon vacancy $V_C$ is the dominant detrimental defect in SiC, and hydrogen passivation of $V_C$ is often used to facilitate its application in electronic devices. However, the exact nature of hydrogen passivation of $V_C$ in 4*H*-SiC remains inconclusive in view of the available divergent experiment and theoretical findings. Here, using the Heyd-Scuseria-Ernzerhof screened hybrid density functional calculations, we demonstrate that the $V_C$ defect can capture up to four hydrogens, and the electrically active levels within the band gap can be entirely passivated, in line with recent reported experimental observations. This paper, thus, casts light on the role of hydrogen passivation in SiC.

DOI: 10.1103/PhysRevMaterials.5.064604

## I. INTRODUCTION

Silicon carbide (SiC) is a wide-band-gap group-IV binary semiconductor that has manifested its potential in applications of high temperature, high power, high-frequency switching, low loss, and harsh environment devices [1,2]. SiC crystallizes in a wealth of polymorphs [3], among which 3*C*, 2*H*, 4*H*, and 6*H* are the well-studied forms. Hexagonal 4*H*-SiC (with space group $P6_3mc$) has been most adopted in actual power devices, given its wide band gap (3.23 eV), high thermal stability, high charge mobility, small anisotropy, as well as the procurability of high-quality crystalline wafers [4–6]. There are two nonequivalent lattice sites, quasihexagonal (h) and quasicubic (k), for both Si and C atoms in 4*H*-SiC.

To improve the on-state performance of 4*H*-SiC power devices, an adequate carrier lifetime is important. The $Z_{1/2}$ [7] and $EH_{6/7}$ [8] intrinsic deep centers are observed to be the dominant lifetime killers [9,10]. Most of the up-to-date investigations have reached a consensus that the carbon vacancy ($V_C$) is the origin for the lifetime killers based on careful correlation analysis among the deep level transient spectroscopy (DLTS) and electron paramagnetic resonance (EPR) measurements [7,8,11–13] in conjunction with theoretical calculations [14–17]. Carbon implantation [18,19], thermal oxidation [20,21], and hydrogen passivation [22,23] are the reported solutions to eliminate the recombination centers and improve the carrier lifetime in SiC. Hydrogen is always an unintentional or intentional impurity in semiconductors due to its natural incorporation during the growth or annealing. It has been used as an element applied to the passivation of defects in diverse materials such as InP [24], GaAs [25], GaN [26], and diamond [27]. Authors of previous theoretical studies on the role of hydrogen in SiC discovered that a trapped hydrogen atom interacts and establishes a three-center bond with two nearest-neighbor Si atoms of the $V_C$ (Si-H-Si) [28,29]. The concept of a three-center bond is quite unusual and counterintuitive since hydrogen normally forms two-center (H-cation or H-anion) bonds in conventional covalent or ionic semiconductors. Indeed, this kind of overcoordinated hydrogen has been found only in a few materials so far, including the inclination of the bond-center site for interstitial H in diamond and silicon [30,31], the B-H-B bonds in the diborane $B_2H_6$ molecule [32], and the fourfold (sixfold) coordinated H substitution on the O site in ZnO (MgO) [33].

Considering the occurrence of the three-center bond of H in SiC, a series of early theoretical works suggested that, when two hydrogens are incorporated with the $V_C$ defect, each H atom respectively binds with two Si neighbors, which prohibits the further trapping of H atom and leads to an incomplete passivation of $V_C$ in SiC [28,29]. However, recent experimental measurements have suggested that the lifetime killer $Z_{1/2}$ center can be totally passivated by hydrogen [22,23]. To address this discrepancy, it is crucial to revisit the nature of hydrogen passivation in SiC.

Note that the previous theoretical studies were based on density functional theory in the local density approximation (LDA), an approach which is well known to severely underestimate the band gaps of semiconductors and fails to accurately predict the localized defect wave functions and defect binding energy [34–36]. More sophisticated functionals beyond the LDA, such as the HSE06 screened hybrid density functional [37], have been found capable of addressing some of the issues of standard LDA and describing the structural and electronic properties of numerous semiconductors more correctly [38]. As such, here, we carefully inspect the hydrogen passivation effect of the $V_C$ defect in 4*H*-SiC by employing the HSE06 functional [37]. Unlike prior studies where at most two hydrogens are considered, here, we consider the sequential interaction behavior of up to four H atoms. Moreover, the ground state geometry for each hydrogen-vacancy ($V_C + n$H) complex is obtained by calculating and comparing the equilibrium total energies of possible configurations. Along with the successive H binding energy and the detailed evolution of single-particle defect levels for all defect complexes under neutral charge state, this paper shows that, in line with the

*hxdeng@semi.ac.cn
†Corresponding author: suhuaiwei@csrc.ac.cn

 ©2021 American Physical Society

recent experimental results, hydrogen can totally passivate the electrically active states of $V_C$ located within the band gap and, therefore, expands the known range of hydrogen passivation behavior of trap centers in semiconductors.

## II. COMPUTATIONAL METHODS

All the calculations were carried out using the projector-augmented wave method and the HSE06 hybrid density functional as implemented in the VASP package [39]. We used a cutoff energy of 520 eV for the plane-wave basis set and a convergence criterion of 10 meV/Å for the Hellman-Feynman force on each atom. A Γ-centered 8 × 8 × 2 Monkhorst-Pack k-point sampling of the Brillouin zone was employed for the unit cell of 4*H*-SiC. The calculated equilibrium lattice parameters for 4*H*-SiC were a = 3.071 Å and $c = 10.051$ Å, in excellent agreement with the experimental data of $a = 3.073$ Å and $c = 10.052$ Å [40]. Additionally, the HSE06 calculation with Hartree-Fock exchange parameter $\alpha = 0.25$ produced a band gap of 3.17 eV compared with the experimental value of 3.23 eV [41].

For defect calculations, we constructed a 4*H*-SiC supercell of 128 atoms and employed a 2 × 2 × 2 Monkhorst-Pack k-mesh for integrations over the Brillouin zone. Since 4*H*-SiC contains two nonequivalent carbon sites, we studied the $V_C$ properties by removing one C atom at either k site or h site from the 128-atom cell, respectively. The defect formation energy and transition energy levels were calculated following the procedure described in the literature [36,42]. The hydrogen atoms were added into the $V_C$ system by forming $V_C + n$H ($n = 1-4$) complexes. Of note is that all the defect systems were optimized within HSE06 with adequate caution to get the lowest energy configurations. Here, we consider only the neutral charge state of each defect complex since our focus is to study the hydrogen passivation effect of the $V_C$ defect in 4*H*-SiC. The spin-polarized calculations were carried out in all the defect systems.

## III. RESULTS AND DISCUSSION

Figure 1 depicts the calculated formation energies for $V_C$(k) and $V_C$(h) defects in 4*H*-SiC as a function of the Fermi level at a C-poor condition. The range of the Fermi level is from the valence band maximum (VBM) to the conduction band minimum (CBM), i.e., from 0 to 3.16 eV in our calculation. Under a C-poor condition, the formation energies are 4.29 eV for neutral $V_C$(k) and 4.42 eV for neutral $V_C$(h), while they are 4.89 and 5.03 eV at a C-rich condition, respectively, which falls in line with the reported experimental measurement of 4.8–5.0 eV [43,44].

For $V_C$ in the negative charge state, the negative-U behavior is found at both k and h sites. The (0/–2) transition energy levels are 0.61 and 0.70 eV below the CBM for $V_C$(k) and $V_C$(h), respectively, with the (0/–) levels lying above (0/–2) by 0.24 eV for $V_C$(k) and 0.11 eV for $V_C$(h). These obtained acceptor levels are in agreement with the reported EPR and DLTS data [11–13], where the (0/–2) level of $V_C$ is correlated with the ∼0.56–0.71 eV level below CBM of $Z_{1/2}$ center, and the (0/–) levels of $V_C$(k) and $V_C$(h) identified as the $Z_1$ (∼0.45 eV) and $Z_2$ (∼0.52 eV) states, respectively.

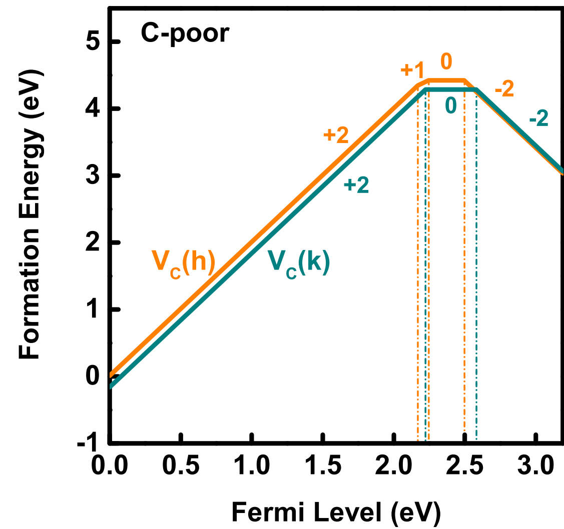


FIG. 1. Formation energies as a function of Fermi level for carbon vacancy at both h-site $V_C$(h) and k-site $V_C$(k) in 4*H*-SiC under C-poor condition. The zero of the Fermi level is at the valence band maximum (VBM) of 4*H*-SiC. The slope of the formation energy segment gives the defect charge state and the Fermi level at which the slope changes denote the transition energy level $\varepsilon(q/q')$.

Additionally, our calculated level separation between (0/–) and (0/–2) for $V_C$(k) is larger than that for $V_C$(h), which is consistent with the experimental observations [11,13]. As shown in Fig. 1, the donor levels of $V_C$ are found to be at 0.95–1.02 eV below the CBM. Although there is difference between these values and the DLTS measurements of $EH_{6/7}$ state at ∼1.40–1.50 eV below the CBM [11,13], resulting probably from the finite supercell size used in our calculation, the hydrogen passivation behavior of $V_C$ in 4*H*-SiC presented below is not affected. Additionally, the discrepancy between our results and previous theoretical findings [14–16] on defect levels of $V_C$ in 4*H*-SiC may be ascribed to the difference in the supercell size, spin-polarization, and optimization procedures. Due to the analogous defect characters between $V_C$(k) and $V_C$(h), we only selected the $V_C$(k) as the representative for the following discussions on $V_C + n$H complex. Thus, if not otherwise specified, $V_C$ refers to $V_C$(k) hereafter.

The relaxed local structure of neutral defect state for single $V_C$ is displayed in Fig. 2(a), where the four nearest-neighbor Si atoms are labeled. Si1 locates on the axial direction [0001], whereas Si2, Si3, and Si4 are the other three atoms within the basal plane. As expected, the four dangling bonds on these Si atoms introduce electrical levels in the band gap, as illustrated in Fig. 3(a). Note that the apparent low-spin state of the charge-neutral $V_C$ defect is in line with the previous observation for the $V_C$ ground state [16,17]. The defect center has a total of $0 + 4 = 4$ electrons, two of which occupied the lowest lying $a_1$ $s$ state, and the remaining two electrons occupy the level in the gap, leaving two empty states close to the CBM.

We now carefully inspect the interaction behavior between $V_C$ and H atoms. Prior theoretical studies have shown that a hydrogen interstitial establishes a three-center bond with two neighboring Si atoms (Si-H-Si) rather than bonds with only one Si (Si-H) [28,29]. Indeed, this bonding character is also

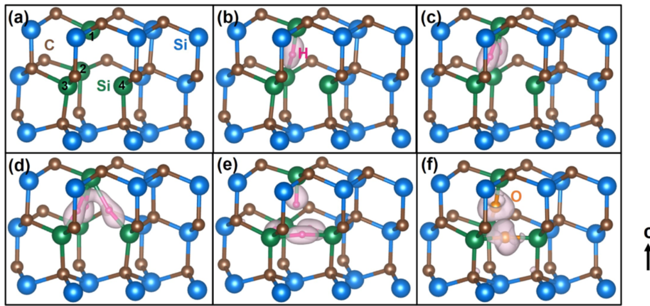


FIG. 2. The stable atomic configuration for neutral defect systems of (a) $V_C$, (b) $V_C + 1H$, (c) $V_C + 2H$, (d) $V_C + 3H$, (e) $V_C + 4H$, and (f) $V_C + 2O$ in 4*H*-SiC. The blue-colored ball is for Si, the brown one is for C, the magenta one is for H, the orange one is for O, and the four Si neighbors of $V_C$ are emphasized in green for convenience. The calculated isosurface plots the charge density difference for H and O incorporation in 4*H*-SiC ($0.01e/\text{Bohr}^3$). The electron charge accumulation is shown in gray areas, whereas the electron depletion is not being displayed for viewing convenience.

observed in this paper [see Fig. 2(b)]. The resulting charge density difference plot apparently exhibits the connecting isosurface in the three-center bond, which reveals the electron sharing of the Si-H-Si pair in the $V_C + H$ system. This can be ascribed to that the distance between two Si neighbors of $V_C$ in 4*H*-SiC (∼3.07 Å) is approximately twice that of the normal Si-H bond length (∼1.5 Å in $SiH_4$). With careful geometry optimizations within HSE06, as shown in Supplemental Material Fig. S1 [45], the defect structure with the Si1-H-Si2 pair is found to be more stable than that with the Si3-H-Si4 pair by 25.3 meV. When a second H atom is captured by the $V_C$, there should be three symmetry-inequivalent configurations for the $V_C + 2H$ complex. It is intuitively expected that the structure with the second H binding to the remaining two neighboring Si atoms of $V_C$ (see Supplemental Material Fig. S2(c) [45]) should be the most stable one. However, this structure turns out to be metastable and, as illustrated in Fig. 2(c), the structure with Si1 bonded with both H atoms turns out to be the ground state with minimum energy.

Turning now to the $V_C + 3H$ complex, similarly, three configurations are considered based on the symmetry arguments. Each fully relaxed atomic geometry and the corresponding energy with respect to the lowest energy one is given in Supplemental Material Fig. S3 [45]. In analogy with the case of the $V_C + 2H$ cluster, all the three hydrogen atoms energetically prefer to connect with one neighbor Si atom (Si1), as displayed in Fig. 2(d). This bonding behavior poses the question: What is the charge state on Si1? By Bader charge analysis [46], we find that the three electrons distribute equally among the four Si atoms close to the $V_C$ defect. That is, the atomic charge of each Si neighbor is ∼+3.75. Next, we examine the $V_C + 4H$ complex in 4*H*-SiC. The calculations obtained at a unique stable configuration shown in Fig. 2(e), where two kinds of H bonding characters coexist: One H solely attaches to one Si neighbor and forms the normal two-center bond (Si-H), whereas the other three hydrogens respectively establish a three-center bond with the other three Si atoms around the $V_C$ defect. Note that, here, we

TABLE I. The successive H binding energy of $V_C + nH$ complex in 4*H*-SiC.

| Defect pair | $V_C + 1H$ | $V_C + 2H$ | $V_C + 3H$ | $V_C + 4H$ |
|---|---|---|---|---|
| $E_b$(eV) | −0.368 | −0.422 | −0.289 | −0.891 |

compared two structures (see Supplemental Material Fig. S4 [45]) considering the symmetry and found only a small energy difference of 15.2 meV between them.

To evaluate the capabilities for energetic capture of the *n*th hydrogen atom in the system, we calculated the binding energy $E_b(V_C + nH)$ ($n = 1-4$) by using the following definition:

$$E_b(V_C + nH) = E(V_C + nH) - E[V_C + (n-1)H] - \frac{E(H_2)}{2}, \quad (1)$$

where $E(V_C + nH)$ and $E[V_C + (n-1)H]$ are the total energies of the supercell with ($V_C + nH$) and $[V_C + (n-1)H]$ complexes, respectively. Here, $E(H_2)$ stands for the energy of the $H_2$ molecule. With such a definition, $E_b(V_C + nH) < 0$ indicates that introducing the *n*th hydrogen atom into the system is energetically favorable. In other words, the $E_b(V_C + nH) < 0$ manifests that it is feasible to add another hydrogen atom into the $[V_C + (n-1)H]$ system. Table I lists the successive H binding energy of $V_C + nH$ complex in 4*H*-SiC. One can see that all the binding energies are negative, which reveal that the *n*th ($n = 1-4$) hydrogen atom can be added to the system. It is worth noting that our results suggest that capturing three or four hydrogens is energetically feasible, which contradicts a previous theoretical prediction using the LDA that the $V_C$ can at most accommodate two H atoms owing to the existence of overcoordinated hydrogen [28,29]. Interestingly, the binding energy of adding the fourth hydrogen atom is more negative than the others. This suggests that, after all four Si are equally passivated by three H with a high-symmetry configuration, the addition of another H prefers to arrive at the same high-symmetry configuration with different two-center and three-center bonds.

Generally, effective defect passivation implies both chemical and electrical passivation, namely, the saturation of the dangling bonds together with the elimination of the electrically active levels within the band gap. To provide a clear picture of the hydrogen passivation process and capabilities, as depicted in Fig. 3(b)–3(e), we plot the evolution of the single-particle defect levels for $V_C + nH$ complexes in the neutral charge state in 4*H*-SiC. When the $V_C$ defect seizes one H, one of the empty levels becomes occupied, as expected. As a second hydrogen is incorporated and the $V_C + 2H$ is formed, despite that the occupied gap levels are overall shifted down compared with those of single $V_C$, two empty states remain basically unaffected inside the band gap, thereby making the complex a donor center, in accordance with the earlier study. Similarly, the $V_C + 3H$ complex is still electrically active with single-particle defect levels occurring inside the band gap. In the case of the $V_C + 4H$ system, all the Si dangling bonds resulting from the $V_C$ defect are completely saturated with the incorporation of four H atoms and the occupied defect levels all moved down and transformed into band edge states

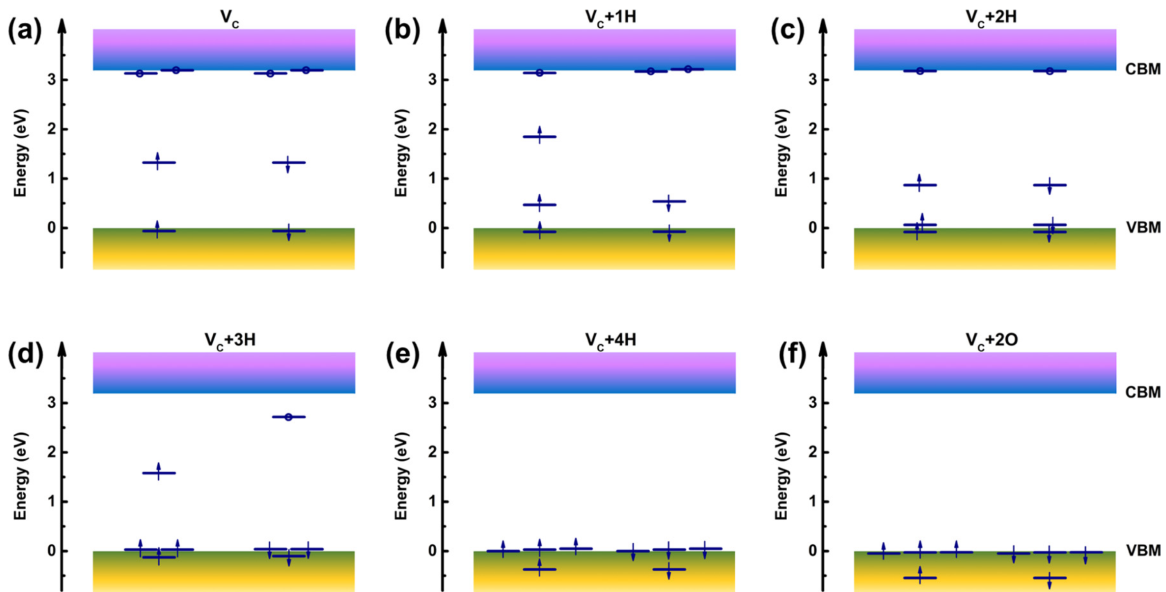


FIG. 3. The single-particle defect levels for $V_C$, $V_C + nH$ ($n = 1 - 4$) and $V_C + 2O$ defects in 4*H*-SiC in the neutral charge state. The upward and downward arrows stand for the up- and down-spin states of the occupied electron, respectively, while the unoccupied hole state is depicted by open dot.

lying in the vicinity of the VBM of host 4*H*-SiC. In short, our calculations demonstrate that the $V_C$ defect in 4*H*-SiC can be effectively passivated by hydrogen.

As noted in the Introduction section, dry oxidation is also a method to passivate the lifetime-killer defect $Z_{1/2}$ center in SiC. Although it is now a general consensus that the mechanism of the thermal oxidation is based on the interstitial diffusion model [20,47], i.e., the oxidizing surface induces and injects carbon interstitials into the SiC bulk interior, leading to the $V_C$ annihilation, we would like to point out that O can also passivate $V_C$ in the 4*H*-SiC bulk. As shown in Supplemental Material Fig. S5 [45], an oxygen atom can bind to two of the Si atoms in the vicinity of the $V_C$ defect, forming the three-center $V_C + 1O$ complex with analogous geometry to $V_C + 1H$. It is interesting to point out that our defect structure search also finds a unique metastable $V_C + 1O$ configuration with the O atom sitting in the $V_C$ site and an energy ~0.44 eV higher than the stable configurations. As a second O is captured by the $V_C$ defect, the oxygen atom interacts with the remaining two Si neighbors by forming another Si-O-Si unit [see Fig. 2(f)]. The different binding characters between H and O incorporating with $V_C$ in 4*H*-SiC can be attributed to the larger atomic radius of the O atom than the H atom and the preferred −2 valence for O. Inspecting the single-particle defect levels of $V_C + 2O$ cluster in 4*H*-SiC, we find it is also an electrically inactive defect complex like $V_C + 4H$.

## IV. CONCLUSIONS

In conclusion, we systematically studied the interaction of hydrogens with a $V_C$ defect in 4*H*-SiC by performing first-principles HSE06 hybrid functional calculations. Our results reveal that hydrogen prefers to form high-symmetry three-center and two-center defect complexes and to passivate all the electrically active levels of $V_C$ within the band gap in 4*H*-SiC by forming the $V_C + 4H$ complex, which is consistent with the recent experimental measurements [22]. Additionally, the $V_C + 2O$ complex is also found to be electrically inactive in 4*H*-SiC. This paper, therefore, provides a more integrated understanding on the passivation behavior of defects in SiC.

## ACKNOWLEDGMENTS

We are grateful for the computational support from the Beijing Computational Science Research Center (CSRC). This paper is supported by the Science Challenge Project (No. TZ2016003 and No. TZ2018004), The Key Research & Development Program of Beijing (Grant No. Z181100005118003), the Nature Science Foundation of China (No. 11634003, No. 11991060, No. 12088101, No. 61922077, No. 11874347, and No. U1930402), the Key Research Program of the Chinese Academy of Sciences (Grant No. XDPB22), and the China Scholarship Council (No. 201904890014). H.-X.D. was also supported by the Youth Innovation Promotion Association of Chinese Academy of Sciences (Grant No. 2017154).

X.C. and Y.Y. contributed equally to this work.

[1] H. Matsunami and T. Kimoto, Step-controlled epitaxial growth of SiC: High quality homoepitaxy, Mater. Sci. Eng. R Rep. **20**, 125 (1997).

[2] J. A. Cooper, M. R. Melloch, R. Singh, A. Agarwal, and J. W. Palmour, Status and prospects for SiC power MOSFETs, IEEE Trans. Electron Devices **49**, 658 (2002).

[3] F. Bechstedt, P. Käckell, A. Zywietz, K. Karch, B. Adolph, K. Tenelsen, and J. Furthmüller, Polytypism and properties of silicon carbide, Phys. Status Solidi B **202**, 35 (1997).

[4] N. Iwamoto and B. G. Svensson, in *Semiconductors and Semimetals* (Elsevier, SanDiego, 2015), p. 369.

[5] S. Chowdhury, C. Hitchcock, R. P. Dahal, I. B. Bhat, and T. P. Chow, in *2016 Lester Eastman Conference (LEC)*, (IEEE, Bethlehem, PA, 2016), pp. 23.

[6] S. H. Ryu *et al.*, Impact of carrier lifetime enhancement using high temperature oxidation on 15 kV 4*H*-SiC *p*-GTO thyristor, Mater. Sci. Forum **897**, 587 (2017).

[7] C. Hemmingsson, N. Son, A. Ellison, J. Zhang, and E. Janzén, Negative-U centers in 4*H* silicon carbide, Phys. Rev. B **58**, R10119 (1998).

[8] C. Hemmingsson, N. T. Son, O. Kordina, J. Bergman, E. Janzén, J. Lindström, S. Savage, and N. Nordell, Deep level defects in electron-irradiated 4*H* SiC epitaxial layers, J. Appl. Phys. **81**, 6155 (1997).

[9] P. B. Klein, B. V. Shanabrook, S. W. Huh, A. Y. Polyakov, M. Skowronski, J. J. Sumakeris, and M. J. O'Loughlin, Lifetime-limiting defects in $n^-$ 4*H*-SiC epilayers, Appl. Phys. Lett. **88**, 052110 (2006).

[10] K. Danno, D. Nakamura, and T. Kimoto, Investigation of carrier lifetime in 4*H*-SiC epilayers and lifetime control by electron irradiation, Appl. Phys. Lett. **90**, 202109 (2007).

[11] N. T. Son *et al.*, Negative-U System of Carbon Vacancy in 4*H*-SiC, Phys. Rev. Lett. **109**, 187603 (2012).

[12] K. Kawahara, X. Thang Trinh, N. Tien Son, E. Janzén, J. Suda, and T. Kimoto, Investigation on origin of $Z_{1/2}$ center in SiC by deep level transient spectroscopy and electron paramagnetic resonance, Appl. Phys. Lett. **102**, 112106 (2013).

[13] X. T. Trinh, K. Szász, T. Hornos, K. Kawahara, J. Suda, T. Kimoto, A. Gali, E. Janzén, and N. T. Son, Negative-U carbon vacancy in 4*H*-SiC: assessment of charge correction schemes and identification of the negative carbon vacancy at the quasicubic site, Phys. Rev. B **88**, 235209 (2013).

[14] T. Hornos, A. Gali, and B. G. Svensson, Large-scale electronic structure calculations of vacancies in 4*H*-SiC using the Heyd-Scuseria-Ernzerhof screened hybrid density functional, Mater. Sci. Forum **679–680**, 261 (2011).

[15] L. Gordon, A. Janotti, and C. G. Van de Walle, Defects as qubits in 3*C*- and 4*H*-SiC, Phys. Rev. B **92**, 045208 (2015).

[16] J. Coutinho, V. J. B. Torres, K. Demmouche, and S. Öberg, Theory of the carbon vacancy in 4*H*-SiC: crystal field and pseudo-Jahn-Teller effects, Phys. Rev. B **96**, 174105 (2017).

[17] X. Yan, P. Li, L. Kang, S.-H. Wei, and B. Huang, First-principles study of electronic and diffusion properties of intrinsic defects in 4*H*-SiC, J. Appl. Phys. **127**, 085702 (2020).

[18] L. Storasta and H. Tsuchida, Reduction of traps and improvement of carrier lifetime in 4*H*-SiC epilayers by ion implantation, Appl. Phys. Lett. **90**, 062116 (2007).

[19] T. Hayashi, K. Asano, J. Suda, and T. Kimoto, Enhancement and control of carrier lifetimes in *p*-type 4*H*-SiC epilayers, J. Appl. Phys. **112**, 064503 (2012).

[20] T. Hiyoshi and T. Kimoto, Elimination of the major deep levels in *n*- and *p*-type 4*H*-SiC by two-step thermal treatment, Appl. Phys. Express **2**, 091101 (2009).

[21] T. Hiyoshi and T. Kimoto, Reduction of deep levels and improvement of carrier lifetime in *n*-type 4*H*-SiC by thermal oxidation, Appl. Phys. Express **2**, 041101 (2009).

[22] T. Okuda, T. Kimoto, and J. Suda, Improvement of carrier lifetimes in highly Al-doped *p*-type 4*H*-SiC epitaxial layers by hydrogen passivation, Appl. Phys. Express **6**, 121301 (2013).

[23] T. Okuda, T. Miyazawa, H. Tsuchida, T. Kimoto, and J. Suda, Enhancement of carrier lifetime in lightly Al-doped *p*-type 4*H*-SiC epitaxial layers by combination of thermal oxidation and hydrogen annealing, Appl. Phys. Express **7**, 085501 (2014).

[24] B. Chatterjee, S. Ringel, R. Sieg, R. Hoffman, and I. Weinberg, Hydrogen passivation of dislocations in InP on GaAs heterostructures, Appl. Phys. Lett. **65**, 58 (1994).

[25] G. Wang, G. Y. Zhao, T. Soga, T. Jimbo, and M. Umeno, Effects of H plasma passivation on the optical and electrical properties of GaAs-on-Si, Jpn. J. Appl. Phys **37**, L1280 (1998).

[26] S. Yagi, Highly sensitive ultraviolet photodetectors based on Mg-doped hydrogenated GaN films grown at 380 °C, Appl. Phys. Lett. **76**, 345 (2000).

[27] K. Czelej and P. Śpiewak, Hydrogen passivation of vacancies in diamond: Electronic structure and stability from *ab initio* calculations, MRS Adv. **2**, 309 (2017).

[28] A. Gali, B. Aradi, P. Deák, W. Choyke, and N. Son, Overcoordinated Hydrogens in the Carbon Vacancy: Donor Centers of SiC, Phys. Rev. Lett. **84**, 4926 (2000).

[29] B. Aradi, A. Gali, P. Deák, J. E. Lowther, N. T. Son, E. Janzén, and W. J. Choyke, *Ab initio* density-functional supercell calculations of hydrogen defects in cubic SiC, Phys. Rev. B **63**, 245202 (2001).

[30] T. Estle, S. Estreicher, and D. Marynick, Preliminary calculations confirming that anomalous muonium in diamond and silicon is bond-centered interstitial muonium, Hyperfine Interact. **32**, 637 (1986).

[31] S. Estreicher, Equilibrium sites and electronic structure of interstitial hydrogen in Si, Phys. Rev. B Condens. Matter. **36**, 9122 (1987).

[32] L. S. Bartell and B. L. Carroll, Electron-diffraction study of diborane and deuterodiborane, Comput. Mater. Sci. **42**, 1135 (1965).

[33] A. Janotti and C. G. Van de Walle, Hydrogen multicentre bonds, Nat. Mater. **6**, 44 (2007).

[34] J. Lægsgaard and K. Stokbro, Hole Trapping at Al Impurities in Silica: A Challenge for Density Functional Theories, Phys. Rev. Lett. **86**, 2834 (2001).

[35] S. Lany and A. Zunger, Polaronic hole localization and multiple hole binding of acceptors in oxide wide-gap semiconductors, Phys. Rev. B **80**, 085202 (2009).

[36] X. Cai, J. Yang, P. Zhang, and S.-H. Wei, Origin of Deep Be Acceptor Levels in Nitride Semiconductors: The Roles of Chemical and Strain Effects, Phys. Rev. Appl. **11**, 034019 (2019).

[37] J. Heyd, G. E. Scuseria, and M. Ernzerhof, Hybrid functionals based on a screened Coulomb potential, J. Chem. Phys. **118**, 8207 (2003).

[38] T. M. Henderson, J. Paier, and G. E. Scuseria, Accurate treatment of solids with the HSE screened hybrid, Phys. Status Solidi B **248**, 767 (2011).

[39] G. Kresse and J. Furthmüller, Efficient iterative schemes for *ab initio* total-energy calculations using a plane-wave basis set, Phys. Rev. B **54**, 11169 (1996).

[40] E. Halac, E. Burgos, and H. Bonadeo, Static and dynamical properties of SiC polytypes, Phys. Rev. B **65**, 125202 (2002).

[41] M. E. Levinshtein, S. L. Rumyantsev, and M. S. Shur, *Properties of Advanced Semiconductor Materials: GaN, AIN, InN, BN, SiC, SiGe* (John Wiley & Sons, New York, 2001).

[42] S.-H. Wei, Overcoming the doping bottleneck in semiconductors, Comput. Mater. Sci. **30**, 337 (2004).

[43] H. M. Ayedh, V. Bobal, R. Nipoti, A. Hallén, and B. G. Svensson, Formation of carbon vacancy in 4*H* silicon carbide during high-temperature processing, J. Appl. Phys. **115**, 012005 (2014).

[44] H. M. Ayedh, R. Nipoti, A. Hallén, and B. G. Svensson, Elimination of carbon vacancies in 4*H*-SiC employing thermodynamic equilibrium conditions at moderate temperatures, Appl. Phys. Lett. **107**, 252102 (2015).

[45] See Supplemental Material at https://link.aps.org/supplemental/10.1103/PhysRevMaterials.5.064604 for the stable and metastable atomic configurations of $V_C + n\mathrm{H}(n = 1 - 4)$ and $V_C + 1O$ complexes in the neutral charge state in 4*H*-SiC.

[46] G. Henkelman, A. Arnaldsson, and H. Jónsson, A fast and robust algorithm for Bader decomposition of charge density, Comput. Mater. Sci. **36**, 354 (2006).

[47] K. Kawahara, J. Suda, and T. Kimoto, Analytical model for reduction of deep levels in SiC by thermal oxidation, J. Appl. Phys. **111**, 053710 (2012).